HHS Public Access

Author manuscript

J Neurochem. Author manuscript; available in PMC 2016 May 01.

Published in final edited form as:

J Neurochem. 2015 May ; 133(3): 452–464. doi:10.1111/jnc.13022.

Substantially elevating the levels of αB-crystallin in spinal motor neurons of mutant SOD1 mice does not significantly delay paralysis or attenuate mutant protein aggregation

Guilian Xu[1,*], **Susan Fromholt**[1,*], **Jacob I. Ayers**[1], **Hilda Brown**[1], **Zoe Siemienski**[1], **Keith W. Crosby**[1], **Christopher A. Mayer**[1], **Christopher Janus**[1], and **David R. Borchelt**[1,†]

[1]Department of Neuroscience, Center for Translational Research in Neurodegenerative Disease, McKnight Brain Institute, University of Florida, Gainesville, Florida 32610

Abstract

There has been great interest in enhancing endogenous protein maintenance pathways such as the heat-shock chaperone response, as it is postulated that enhancing clearance of misfolded proteins could have beneficial disease modifying effects in ALS and other neurodegenerative disorders. In cultured cell models of mutant SOD1 aggregation, co-expression of αB-crystallin (αB-crys) has been shown to inhibit the formation of detergent-insoluble forms of mutant protein. Here, we describe the generation of a new line of transgenic mice that express αB-crys at >6-fold the normal level in spinal cord, with robust increases in immunoreactivity throughout the spinal cord grey matter and, specifically, in spinal motor neurons. Surprisingly, spinal cords of mice expressing αB-crys alone contained 20% more motor neurons per section than littermate controls. Raising αB-crys by these levels in mice transgenic for either G93A or L126Z mutant SOD1 had no effect on the age at which paralysis developed. In the G93A mice, which showed the most robust degree of motor neuron loss, the number of these cells declined by the same proportion as in mice expressing the mutant SOD1 alone. In paralyzed bigenic mice, the levels of detergent-insoluble, misfolded, mutant SOD1 were similar to those of mice expressing mutant SOD1 alone. These findings indicate that raising the levels of αB-crys in spinal motor neurons by 6-fold does not produce the therapeutic effects predicted by cell culture models of mutant SOD1 aggregation.

[†]To whom correspondence should be addressed: David R. Borchelt, Department of Neuroscience/CTRND, Box 100159, University of Florida, Gainesville, FL 32610, USA, Tel.: (352) 273-9664; drb1@ufl.edu.

[*]These authors contributed equally to this work.

Conflict-of-interest disclosure

The authors declare that they have no competing interests.

Supporting Information

Additional supporting information may be found in the online version of this article at the publisher's website:

Figure S1. Amino acid sequence alignment of mouse and human αB-crys.

Figure S2. Quantification of αB-crys levels in αB-crys (Z104) transgenic mice.

Figure S3. αB-crys does not exclusively co-localize with ubiquitin immunoreactive aggregates in spinal cords of paralyzed bigenic mice.

Figure S4. αB-crys does not exclusively co-localize with SOD1 immunoreactive inclusions in spinal cords of paralyzed bigenic mice.

Figure S5. Effect of αB-crys over-expression on the oligomerization of G93A and L126Z mutant SOD1 in cultured cells.

Figure S6. Captured image of in situ hybridization for αB-crys mRNA in the brains of young C57BL/6J mice (www.brain-map.org).

Figure S7. Captured image of in situ hybridization for αB-crys mRNA in the spinal cords of young C57BL/6J mice (www.brain-map.org).

Keywords

amyotrophic lateral sclerosis; superoxide dismutase 1; protein aggregation; chaperones; proteostasis

Introduction

The accumulation of misfolded proteins in degenerating motor neurons is a hallmark of both familial and sporadic amyotrophic lateral sclerosis (ALS) (Mulligan and Chakrabartty 2013). In familial ALS (fALS) caused by mutations in superoxide dismutase 1 (SOD1), the accumulation of misfolded mutant SOD1 has been demonstrated in humans and multiple model systems (Bruijn *et al.* 1997; Johnston *et al.* 2000; Jonsson *et al.* 2004; Karch *et al.* 2009; Prudencio *et al.* 2009; Prudencio and Borchelt 2011; Wang *et al.* 2002a; Wang *et al.* 2002b; Wang *et al.* 2003; Wang *et al.* 2005a; Wang *et al.* 2005b; Watanabe *et al.* 2001). Sporadic forms of ALS parallel familial disease in that ubiquitinated inclusion pathology has long been recognized as a common feature (Lowe *et al.* 1993). More recently, additional protein components of these inclusions have been suggested by immunoreactivity of such inclusions with antibodies to SOD1, TDP-43 and, or, ubiquilin (Bosco *et al.* 2010; Deng *et al.* 2010; Deng *et al.* 2011; Fecto and Siddique 2011; Forsberg *et al.* 2010; Grad *et al.* 2014). The prevalence of these proteinaceous inclusions in diseased tissue from sporadic ALS patients can be viewed as evidence that the systems responsible for maintaining protein homeostasis and preventing protein aggregation have been compromised (Balch *et al.* 2008; Morimoto 2008). Thus, there has been great interest in enhancing endogenous protein maintenance pathways such as the heat-shock chaperone response.

Heat shock proteins (HSPs) are one of the major protein chaperone systems responsible for proper folding of newly synthesized proteins, also playing major roles in clearance of both misfolded and aggregated proteins [for reviews see (Frydman 2001; Sherman and Goldberg 2001)]. Although there are constitutively expressed HSPs, cellular responses to stresses, such as increased temperature that results in increased protein misfolding and aggregation, typically induce a dynamic up-regulation of the HSP40/HSP70 class of chaperones. The up-regulation of these effector HSPs is mediated by activation of the transcription factor heat-shock-factor 1 (HSF1) [for review see (Akerfelt *et al.* 2010)]. However, unlike many other types of cells studied to date, it is clear that in most neurons the heat shock response to both classic stressors and pharmacologic inducers is blunted (Batulan *et al.* 2003; Kaarniranta *et al.* 2002; Oza *et al.* 2008; Pavlik *et al.* 2003; Rangaraju *et al.* 2008; Vogel *et al.* 1997; Yang *et al.* 2008) [for review see (Pavlik and Aneja 2007)]. In general, the regulation of the heat-shock response in neurons remains poorly understood.

Despite the hurdles to modulating chaperones in the nervous system, several efforts have pursued manipulating the chaperone response in central nervous system using compounds such as resveratrol, a natural phenol derived from various plants including the Japanese Knotweed. This drug potently induced expression of HSP25 in the spinal cords of the G93A mouse model of SOD1-linked ALS (fold induction not quantified but estimated to be >3 fold) (Han *et al.* 2012). Unfortunately, the effects of resveratrol on the age to paralysis of the

G93A model of SOD1-linked ALS were very modest (about a 14 day delay) and a detailed description of the types of CNS cells that responded to the drug was not provided. Arimoclomol, a synthetic small molecule that induces chaperone expression, has been shown to delay disease onset and extend survival of G93A mice by 2–3 weeks (Kieran *et al.* 2004). The drug was later also shown to prevent declines in HSP70 levels that occur in the G93A SOD1 mice as they develop motor neuron disease (Kalmar *et al.* 2008). Arimoclomol induced HSP70 expression by 3-fold overall and there was histologic evidence of a response in motor neurons (Kieran *et al.* 2004). Arimoclmol is currently under investigation in Phase II/III clinical trials for ALS.

Several investigators have used genetic strategies as a means to increase chaperone expression in mouse models of SOD1-linked ALS, including direct expression of HSP70, expression of HSF1, and expression of other small chaperones. Mice that over-express HSP70 at levels approaching 10 times the normal level have been crossed to mice that express three different fALS mutants of SOD1, G37R, G85R, and G93A, producing bigenic mice that showed no statistically significant delay in age to paralysis (Liu *et al.* 2005). In these mouse models, some of the induced HSP70 was found to be co-localized with SOD1 immunoreactive inclusion structures in neuropil, but it was not clear which cell types over-produced the bulk of the over-expressed HSP70. The promoter element for the transgene in the HSP70 mice used by Liu et al was derived from the chicken beta actin gene (Marber *et al.* 1995). Induction of HSP40/70 in spinal cords of G93A SOD1 mice, by 2–3 fold, has been demonstrated by transgenic over-expression of HSF1 (Lin *et al.* 2013), using a transgene vector that expresses in both neurons and astrocytes. This report did not provide histologic evaluation of which cells responded to the added HSF1 expression. Although Line et al reported that the age at which mice that were bigenic for the G93A mutant SOD1 and HSF1 first developed symptoms was later than that of mice that express the G93A mutant alone, on the whole, the average age to paralysis for bigenic mice was not statistically different from that of mice expressing SOD1-G93A alone (Lin *et al.* 2013). Collectively, these studies provide a mixed view of the potential efficacy of inducible HSPs in ameliorating the phenotypes caused by expression of mutant SOD1.

In previous work, we have observed that the small HSP known as αB-crys can, when over-expressed, diminish the ability of mutant SOD1 to form detergent insoluble aggregates in vitro (Wang *et al.* 2005a) and in cell culture models (Karch and Borchelt 2010). αB-crys is normally induced in mutant SOD1 mice that develop paralysis, with immunoreactivity to this protein being prominent in astrocytes and oligodendrocytes (Wang *et al.* 2005a). Genetic ablation of αB-crys in mice expressing either the G37R or L126Z mutant of SOD1 produced small, but statistically significant, reductions in the age to paralysis for these mice (Karch and Borchelt 2010). On the basis of these prior findings, we launched an effort to genetically increase αB-crys levels in spinal motor neurons for the purpose of crossing these mice to mouse models of SOD1-linked fALS. We here report that we produced mice that show increased levels of αB-crys (~6-fold) in total spinal cord homogenates with robust increases in immunoreactivity throughout the spinal cord grey matter and specifically in spinal motor neuron. Mice bigenic for the αB-crys genes and genes for either G93A or L126Z mutant SOD1 developed paralysis at ages only slightly later than that of mice

expressing the mutant proteins alone. These findings provide an additional perspective on the potential efficacy of chaperone induction in modulating SOD1 misfolding and aggregation *in vivo*.

Materials and Methods

Transgenic Mice

The αB-crys transgenic mice were generated by inserting the cDNA for human αB-crys into the XhoI site of the Mo.PrP.Xho vector (Borchelt *et al.* 1996). This vector consists of a 6 kb promoter element of the mouse *prnp* gene, the first exon, the first intron, and then fused elements of the 2nd and 3rd exon to eliminate all prion (PrP) protein coding sequence, which is not interrupted by introns and is positioned in the 3rd exon. In this vector, the cDNA for αB-crys replaces the coding sequence for PrP. Other modifications include optimization of the Kozak sequence for translation initiation (Kozak 1987). The linearized PrP.αB-crys construct was injected into fertilized embryos of C3/B6 F2 hybrid mice. Founders were identified by PCR of DNA isolated from tail biopsy using the following primers: PrP-SJ—GGG ACT ATG TGG ACT GAT GTC GG; PrP-ASJ—CCA AGC CTA GAC CAC GAG AAT GC; and αBcrys-S1—ATG GAC ATC GCC ATC CAC C.

Lines of SOD1 expressing mice that were used in this study included mice expressing the G93A hSOD1 developed by Gurney et al. (Gurney *et al.* 1994), and L126Z-SOD1- line 45 mice described by Wang et al (Wang *et al.* 2005a). For all previously described strains of mice, animals were bred in house and identified by PCR amplification of DNA extracted from tail biopsies as described in prior descriptions of the animals. All lines of mice used in this study were maintained by crossing transgenic males to non-transgenic (C57BL/6J × C3/HeJ F1) females (Jackson Laboratories, ME). Note that the Gur1-G93A line of mice was also bred to B6/C3 F1 females (>10 generations), which switched the background strain of these mice from B6/SJL to B6/C3 so that all lines of mice would be on the same background. All procedures involving animal handling and processing were approved by the University of Florida Institutional Animal Care and Use Committee, following guidelines set forth by the National Institutes of Health.

Neuropathologic studies

All the mice were euthanized by exsanguination and perfusion with phosphate buffered saline (PBS) under isoflurane anesthesia. After the brain and spinal column were removed, one hemibrain and half of the spinal cord segments were frozen on dry-ice for biochemical analysis. The other hemibrain and segments of the spinal column were immersion fixed in 4% of paraformaldehyde in PBS at 4°C for 48 hours, then were stored in PBS at 4°C until processed for sectioning. Spinal cords were carefully dissected from spinal columns. The tissues were embedded in paraffin and sectioned at 5 μm, sampling randomly through different levels of the spinal cord. Immunohistochemical, immunofluorescence and Thioflavin S staining of paraffin sections were performed according to standard protocols as previously described (Wang *et al.* 2005a). The antibodies used include a rabbit polyclonal antibody to ubiquitin (1:500, DAKO, CA), an antibody to αB-crys (1B6.1-3G4, 1:500, mAb, Enzo, NY), wSOD1 [1:200, a rabbit antiserum raised against full length SOD1 protein

(Ratovitski *et al.* 1999)], and C4F6, a mouse monoclonal antibody against G93A SOD1 (1:200, MédiMabs, Montréal Québec, CANADA). An Olympus DSU-IX81 spinning disc microscope and an Olympus BX60 epi-fluorescence microscope were used to capture the fluorescent images. All the standard light images were captured on an Olympus BX60 microscope.

Spinal cord sections from 5–15 animals per genotype [NTg, Z104, SOD1 G93A, SOD1-G93A × Z104, SOD1-L126Z (line 45), SOD1-L126Z (line 45) × Z104] were used for motor neuron counting. For each animal, we analyzed 2–3 slides, with each slide containing 2–4 spinal cord coronal sections from different regions of the cord. All the sections were 5 μm thick, motor neurons were immunostained with a goat anti-choline acetyltransferase (ChAT) antibody (1:200, Millipore, MA). The stained slides were scanned by Aperio® XT System (Leica Biosystems). Two independent observers, blinded to genotype, counted ChAT immunoreactive cells in spinal cord twice. The numbers for each animal were averaged and used to estimate the average number of motor neurons per section per animal by genotype.

Immunoblotting for αB-crys and SOD1

To measure the levels of αB-crystallin in brain, spinal cord, and other tissues, in both transgenic and non-transgenic (NTg) mice, animals were euthanized by exsanguination and perfusion with PBS under anesthesia. The brain, spinal cord and some other organs were removed and frozen on dry-ice. The tissues were weighed and homogenized in 10 volumes of PBS with protease inhibitor cocktail (Sigma, St. Louis, MO, USA) on ice. The homogenates were centrifuged at 3,000rpm (800×g) for 10 minutes, then the supernatants were mixed with equal volume of 2× Laemmli buffer. Five microliters (5 μl) of each sample was loaded on 18% Tris-glycine gel for western blot. wSOD1 (1:2000) and αB-crys (1:2000) antibodies were used together in immunoblotting, with the SOD1 antibody serving to demonstrate equivalent loading by detecting endogenous mouse SOD1.

The procedures used for assessing the levels of detergent insoluble SOD1 and αB-crys by detergent extraction and centrifugation were similar to work previously described (Karch and Borchelt 2010). Brain or spinal cord tissues were held on ice and sonicated 3 times for 10 s each in 1× TEN buffer (10 mM Tris, pH 7.5; 1mM EDTA, pH 8.0; 100 mM NaCl) containing 1:100 v/v protease inhibitor cocktail, followed by centrifugation at 800 ×*g* for 10 min. The resulting supernatants were mixed with 10%NP-40 to a final concentration of 0.5%, sonicated briefly, and centrifuged at 100,000*g* for 5 min. The resulting supernatant was kept as S1. Pellets were resuspended in 1× TEN buffer with 0.5% NP-40 by sonication and centrifuged at 100,000*g* for 5 min. Supernatant was removed, and the pellet was resuspended in water, sonicated, and kept as P2. The protein concentrations of the S1 and P2 fractions were then determined by bicinchoninic acid assay, as described by the manufacturer (Pierce Biotechnology). Five micrograms (5 μg) of the S1 fractions and 20 μg of the P2 fractions were boiled for 5 min in Laemmli sample buffer with β-mercaptoethanol for sodium dodecyl sulfate-polyacrylamide gel electrophoresis (SDS-PAGE), and electrophoresed in 18% Tris-Glycine gels (Invitrogen/Life Technologies, Carlsbad, CA). Following transfer, membranes were blocked in 5% milk in phosphate-buffered saline (PBS)-T (1× PBS, 0.1% Tween-20) for 20–30 min then incubated for 1 h at room

temperature or overnight at 4°C with a rabbit polyclonal antibody to SOD1 (Ratovitski *et al.* 1999) or a mouse monoclonal antibody to αB-crys (1:2000). The membrane was then washed with PBS-T, incubated for 1 h at room temperature with a goat anti-rabbit or a goat anti-mouse IgG secondary antibody at 1:5000 in PBS-T and 5% milk before developing with enhanced chemiluminescence reagents (Thermo Scientific Inc., Rockford, IL, USA) and visualizing with a FluorChem E imager (Protein Simple, Santa Clara, CA, USA). The intensity of immunoreactive bands on the blots was quantified using software provided with the imaging device. The units of measure are arbitrary units of pixel intensity within the volume of the band (outlined with a box of the same size for each band).

Blue-Native-Gel-Electrophoresis (BNGE) and immunoblotting

The protocol utilized was provided by the supplier of Blue-Native gels after the publication by Shagger and von Jagow (Schagger and von Jagow 1991). HEK 293FT cells (Invitrogen/ Life Technologies), were transfected using Lipofectamine 2000 according to the manufacturer's protocol. The total amount of DNA was kept constant regardless of whether there were one or two plasmids. After 24 hours, cells were rinsed with 10 mM Tris-HCl, pH 7.4, harvested by pipetting using a large bore tip in 50 mM Bis-Tris, 16 mM HCl, 50 mM NaCl, and centrifuged at 3000×g for 2 minutes. The cell pellet was resuspended in the above buffer plus 1% Digitonin and mixed on the Nutator for 30 min at RT. The lysed cells were pelleted at 3000×g for 2 minutes. The supernatant (S1) was centrifuged in an Airfuge for 5 min. This supernatant (S2) was mixed with 4× Sample NativePAGE sample buffer (Life Technologies, BN 2003) and G-250 sample additive (Life Technologies, BN 2004) and run on 3–12% Bis-Tris gel with Dark Blue Cathode buffer at 150 v for 45 min, with Light Blue Cathode Buffer at 150v for 15 min and with Light Blue Cathode buffer at 250 v for 1 hour, according to Invitorgen/Life Technologies' NativePAGE gel protocols. The protein was transferred to PVDF and fixed on the membrane by drying overnight before the membrane was destained in methanol and then rinsed in water before immunoblotting with the hSOD antibody [described in (Bruijn *et al.* 1997)].

To prepare extracts of spinal cord for BNGE, tissues were dounce homogenized to a 10% w/v homogenate in 50 mM Bis-Tris, 16 mM HCl, and 50 mM NaCl containing 1:100 v/v protease inhibitor cocktail (Sigma, St. Louis, MO). Digitonin was then added to 0.5% for each sample, incubated with rocking at room temperature for 30 min and then centrifuged at 3000×g for 2 minutes. The supernatant (S1) was spun in the airfuge for 5 min. This supernatant (S2) was mixed with 4× Sample NativePAGE sample buffer (Life Technologies, BN 2003) and G-250 sample additive (Life Technologies, BN 2004) and run on 4–16% Bis-Tris gels and transferred to PDVF as described above before immunoblotting with the hSOD1 antibodies [described in (Bruijn *et al.* 1997)].

Statistical Methods

The probability of survival (or in the specific use here, age to paralytic humane endpoint) was assessed by the Kaplan-Mayer technique, which computes the probability of survival at every occurrence of death. The technique is particularly suitable for smaller sample size cases with variable event intervals. The comparisons of cumulative survival curves were performed using Gehan-Breslow-Wilcoxon test (GraphPad PRISM 5.01 Software, La Jolla,

CA). The statistical analysis of immunoblot data was done using Student's *t*-test (2-tailed, preceded by Leven's test for equal variance). The analysis of ChAT positive motor neurons in spinal sections were analyzed by assessing departures from normal distribution, using Kolmogorov-Smirnov (K-S) goodness of fit test. A general linear model of factorial ANOVA (Statistical Package for Social Sciences, SPSS v.22, Inc. Chicago), with genotype (non-Tg, Z104, G93A and L126Z (Line45)), and number of neurons as between- subjects factors was used to analyze the data. When necessary, degrees of freedom were adjusted by Greenhouse-Geisser epsilon correction for the heterogeneity of variance. Bonferroni adjustment of α-level (MODLSD Bonferroni t-tests, SPSS v22) was applied in multiple planned comparisons. Comparisons between two independent groups were done using Student t-test, with a Bonferroni Inequality correction whenever multiple comparisons were performed. The critical α-level was set to at least 0.05 for all analyses.

Results

After an initial screening of founder mice derived from embryos injected with the PrP.αB-crys construct, two were identified that possessed strong PCR signals in analysis of tail biopsy DNA (not shown). To assess the levels of αB-crys in CNS tissues, we probed immunoblots of tissue homogenates with a previously described commercial antibody to αB-crys (Karch and Borchelt 2010; Wang *et al.* 2005a). This antibody shows strong reactivity to mouse αB-crys, and because human and mouse αB-crys differ at only 3 amino acid residues, at 3 very distinct locations (Fig. S1), we can be reasonably confident that the avidity of the antibody for human and mouse αB-crys is similar. One of the two lines of mice, designated Z104, showed relatively strong expression of αB-crys in forebrain, cerebellum, and spinal cord (Fig. 1A). Quantification of αB-crys levels in brain and spinal cord indicated that the steady state levels of this chaperone were raised by ~30 fold in the forebrain and ~6 fold in spinal cord (Fig. S2). Expression of endogenous αB-crys in muscle was relatively high and it was not clear whether the levels were consistently elevated in the transgenic mice. Obvious increased expression was evident in the kidney, with no evidence of expression in lung, spleen, testes, or liver. Immunostains of spinal cord sections from the Z104 αB-crys mice demonstrated a robust increase in immunoreactivity in spinal motor neurons (Fig. 1B). These high levels of expression produced no obvious phenotypic traits; mice from the Z104 line were indistinguishable from non-transgenic littermates in home cage behavior and appearance, there was no indication of abbreviated lifespan, and brain/spinal cord morphology was normal (not shown). Although we would have liked to have identified more highly expressing lines of mice to analyze further, we decided that raising the levels of αB-crys by 6 fold in spinal cord (probably more in motor neurons) could provide a reasonable test of whether increasing the levels of this specific chaperone could have significant impact on neuronal proteostasis and prevent mutant SOD1 aggregation.

To determine whether expression of αB-crys, at the levels achieved in the Z104 line of mice, may delay the age at which mutant SOD1 causes motor neuron disease, we mated the Z104 mice to mice that express the G93A and L126 variants of hSOD1. The G93A line we used was derived from the Gur1 strain, which was originally created in the B6/SJL hybrid strain of mice. To standardize the G93A mice with strains of mice we have studied that were created in the B6/C3H background, we crossed male Gur1 G93A transgene positive mice to

B6/C3H F1 female mice and then successively crossed the resulting transgene positive males of each generation to B6/C3H F1 females for 10 generations. The resulting substrain of Gur1-G93A mice that we cultivated develops paralysis at ~6 months of age (Fig. 2). Bigenic offspring of Gur1-G93A-B6C3 mice and Z104 mice developed paralysis at approximately the same age (Fig. 2). Both Log-rank (Mantel-Cox) Test (p=0.40) and Gehan-Breslow-Wilcoxon Test (p=0.50) statistical analysis showed no significant difference in age to paralysis [Median survival G93A (n=6), 171.5 days, G93A × Z104 (n=14), 179.0 days]. We also mated Z104 mice to SOD1-L126Z-line 45 (Wang *et al.* 2005a) mice to create bigenic animals. Mice expressing SOD1-L126Z alone developed paralysis at ~8 months of age (n=11, median: 240 days) and the bigenic mice developed paralysis at approximately the same age (n=9, median: 261 days, log-rank test p=0.92, and Gehan-Breslow-Wilcoxon test p=0.43) (Fig. 2).

To determine whether the increased levels of αB-crys reduced motor neuron loss, without affecting the age to paralysis, we used immunostaining with ChAT to identify motor neurons in the ventral horn of the spinal cord (Fig. 3A) and quantify them by counting the number of positive neurons in the ventral horn of the spinal cord in randomly selected sections (see Materials and Methods, Fig. 3B). The number of ChAT positive neurons for each section where then averaged for each individual animal and the data were statistically analyzed on the basis of an *n* equal to the number of animals for each genotype. In mice expressing αB-crys, alone, we unexpectedly observed ~20% more ChAT immunoreactive motor neurons per spinal cord than non-transgenic littermates (t-test, p=0.048). As expected, paralyzed mice from the G93A line showed fewer ChAT positive motor neurons (p=0.013), but the number of ChAT positive neurons in paralyzed bigenic G93A/αB-crys mice was significantly higher (p=0.016), being statistically similar to that of non-transgenic littermates (p=0.47) (Fig. 3B). These data indicate that αB-crys may be a developmental neuroprotective factor [similar to manipulations that inhibit apoptotic cell death such as deletion of BAX (Gould *et al.* 2006)] by attenuating developmental motor neuron death and raising the total number of motor neurons. In such a setting, it is hard to definitively conclude αB-crys expression was neuroprotective against mutant SOD1 toxicity because the number of motor neurons per section in the bigenic G93A/αB-crys mice was lower than that of mice expressing αB-crys alone (Z104 mice) (two tailed t-test, $p<0.01$).

Although the SOD1-L126Z-Line 45 mice have been in existence since 2005 (Wang *et al.* 2005a), there had not been a detailed study of motor neuron numbers in this line of mutant SOD1 mice. In this first assessment of motor neuron pools, we observe that sections of spinal cords from paralyzed SOD1-L126Z mice – Line 45 have approximately the same number of ChAT positive motor neurons at the time of paralysis as asymptomatic non-transgenic littermates (Post Hoc Test, p=0.15). Consequently, the number of ChAT positive motor neurons per section in paralyzed bigenic L126Z/αB-crys mice were also similar to that of non-transgenic littermates (Post Hoc Test, p=0.46, respectively). Collectively, these data do not support the conclusion that raising αB-crys levels provided significant protection from mutant SOD1 toxicity.

To assess whether expression of αB-crys may have diminished the aggregation of mutant SOD1 without affecting the course of disease, we subjected spinal cords of paralyzed mice

to detergent extraction and sedimentation fractionation as previously described (Karch *et al.* 2009). Immunoblots of these fractions were probed with an SOD1 antibody raised against the whole denatured protein (Ratovitski *et al.* 1999). In soluble fractions from these mice, as previously reported (Wang *et al.* 2005a), it was difficult to detect the L126 truncation product; instead we detected only the endogenous mouse SOD1 protein (Fig. 4A, arrow). As expected from previous study (Wang *et al.* 2005a), the detergent insoluble fractions (NP40) from paralyzed mutant mice contained significant amounts of insoluble mutant SOD1, with some of this protein migrating at higher than expected molecular weight (Fig. 4B, lanes 5–10). In previous work, we have determined that some of these higher molecular weight bands are ubiquitinated protein (Wang *et al.* 2005a). Notably, there was no obvious difference in the amount of insoluble mutant protein in Line 45/Z104 bigenic relative to the Line 45 mice (Fig. 4B, lanes 8–10, p=0.18 –panel to the right). Immunoblots of soluble fractions with antibody to αB-crys demonstrated that the overall levels of this small chaperone were elevated in mice harboring the PrP.αB-crys transgene (Fig. 4C, lanes 3, 4, 8–10, $p<0.05$ – panel to the right). In the insoluble fractions, we observed that increasing the overall expression of αB-crys increased the amount of this protein that became detergent insoluble (Fig. 4D, lanes 3 and 4, $p<0.05$ – panel to the right). As previously reported (Wang *et al.* 2005a), spinal cords of paralyzed mice expressing mutant SOD1 contained higher levels of insoluble αB-crys (Fig. 4D, lanes 5–7). Here, the levels of insoluble αB-crys closely approximated the levels in transgenic mice that over-expressed αB-crys alone (Fig. 4D, compare lanes 3 and 4 to 5–7, p=0.15 – panel to the right). In paralyzed bigenic mice, there was a slightly higher level of insoluble αB-crys as compared to either the Line 45 mice or the Z104 mice (Fig. 4D, lanes 8–10, $p<0.05$ panel to the right). Overall, we observed no clear effect of over-expressed αB crys on the levels of insoluble SOD1-L126Z in paralyzed bigenic mice.

A very similar picture emerged when we analyzed the levels of soluble and insoluble SOD1-G93A in bigenic mice (Fig. 5). Co-expression of αB-crys with SOD1-G93A had no obvious effect on the levels of soluble (Fig. 5A) or insoluble (Fig. 5B, p=0.11- panel to the right) mutant protein. Similarly, we observed a similar pattern of changes in the levels of αB-crys in soluble and insoluble fractions from these mice (Fig. 5C and D; quantification in the panels to the right). The levels of αB-crys in bigenic mice were significantly higher than either of the single transgenic mice (Fig. 4D, $p<0.01$- panel to the right).

Pathologic analyses of inclusion pathology in the G93A and L126Z mice confirmed our data from biochemical assessments of mutant SOD1 aggregation. To specifically detect inclusion pathology in the G93A mice, spinal cord sections were immunostained with antibodies to ubiquitin and stained histologically with thioflavin S to reveal inclusion pathology. As compared to non-transgenic mice or Z104 mice that express αB-crys alone (Figs. 6A and B), mice that express SOD1-G93A show punctate ubiquitinated inclusions throughout the neuropil (Fig. 6C). In bigenic G93A/αB-crys mice, the relative abundance of ubiquitinated inclusions was not obviously different (Fig. 6D). Similarly, the relative abundance of thioflavin-S positive inclusions in mice expressing mutant SOD1 alone was similar to that of bigenic mice (Figs. 6E and F). In mice that express SOD1-L126Z, all detectable mutant protein is found in inclusions, and these structures are readily revealed with immunostaining

using the C4F6 antibody (Xu *et al.* 2014). Bigenic mice co-expressing L126Z SOD1 and αB-crys showed similar levels of C4F6 immunoreactive inclusion structures (Figs. 6G and H). Overall, we could find no obvious effect of co-expressed αB-crys on the degree of inclusion pathology.

In our biochemical analyses of SOD1 and αB-crys, we noted that in mutant mice a substantial fraction of the αB-crys immunoreactivity fractionated to the detergent insoluble fraction (see Figs. 4C and 5C, lanes 3 and 4 of each). Changes in the detergent solubility of αB-crys have been described as a property of this protein when expression is induced (Kumar and Rao 2000). To determine whether any of the insoluble αB-crys was associated with aggregates of mutant SOD1, we co-stained sections of bigenic mice with antibodies to αB-crys and SOD1, or ubiquitin (Figs. S3 and S4). Although there were clear examples of inclusion containing cells that expressed αB-crys, there was little evidence of specific co-localization. Moreover, there were clear examples of inclusions that did not stain for αB-crys in these images. Thus, we cannot easily conclude that the majority of detergent-insoluble αB-crys was sequestered into mutant SOD1 aggregates. Instead, we conclude that the inherent propensity of this protein to oligomerize into detergent insoluble structures (Kumar and Rao 2000) is likely to account for the high levels of αB-crys in detergent insoluble fractions from the paralyzed bigenic.

In prior studies, we have demonstrated that the formation of detergent-insoluble aggregates of SOD1 in transiently-transfected HEK293FT cells can be attenuated by co-expressing αB-crys (Karch and Borchelt 2010). We have recently developed methods of detecting soluble forms of mutant SOD1 that appear to be assembled into multimeric structures by BNGE (Brown and Borchelt 2014). We reasoned that if the high molecular weight smears seen in immunoblots of BNGE are oligomeric assemblies of mutant SOD1, then we might be able to specifically inhibit their formation by co-expression of αB-crys. To assess whether the formation of putative soluble oligomeric forms of mutant SOD1 is attenuated by co-expression of αB-crys, we used both cell culture and mouse models. First, using the HEK293FT cell model, we observed soluble forms of mutant SOD1 that migrated at higher molecular weights than WT SOD1. For the G93A variant, we detect a broad band that migrated more slowly than WT SOD1 along with a smear of higher molecular weight reactivity [Figs. S5 A and B shows the range of outcomes, also see (Brown and Borchelt 2014)]. Similarly, we observed higher than expected molecular weight bands in cells expressing the L126Z variant along with a smear of much higher molecular weight material (Figs. S5A and B)(Brown and Borchelt 2014). If αB-crys were specifically inhibiting oligomeric assembly of mutant SOD1, then we might expect to either see a collapse of the high molecular weight smear into a single entity that co-migrated with WT-hSOD1, or the appearance of a new band caused by the stable association of αB-crys with mutant SOD1. However, we observed neither of these outcomes. Instead, we observed as diminished reactivity for all forms of SOD1 in lysates of cells co-expressing αB-crys (Figs. S5 A and B). Immunoblots of SDS-PAGE from the same lysates did not indicate that the levels of SOD1 in the co-transfected cells were markedly lower than that of cells expressing the mutant SOD1 alone (Figs. S5, C and D). Additionally, although overall reactivity was diminished by co-expression of αB-crys, it was still possible to detect higher molecular

weight SOD1 entities in lysates of cells expressing either G93A or L126Z-hSOD1 (Figs. S5A and B, lanes 5, 6 and 7, 8). At present, we cannot explain the overall diminished SOD1 immunoreactivity in immunoblots of BN-gels, but we are not inclined to conclude that the co-expressed αB-crys produced any reproducible effect on multimerization.

Using this same system to examine soluble forms of SOD1 in the L126Z and L126Z × αB-crys bigenic mice, we observed an array of soluble high molecular weight forms of mutant SOD1 that migrated much more slowly than purified WT human SOD1 (Fig. 7). In bigenic mice, the overall levels of L126Z immunoreactivity of all sizes was diminished (Fig. 7). However, there was such variability in the levels of slowly migrating SOD1 immunoreactivity that we could not measure a statistically significant decrease in high-molecular-weight SOD1 immunoreactivity in the bigenic mice (Fig. 7, p=0.11, comparing L45 to L45 × Z104). We conclude that expressed αB-crys was not able to consistently diminish mutant SOD1 oligomerization *in vivo*.

Discussion

Over the past ten years, there has been significant effort towards determining whether manipulation of the proteostasis network could provide disease modifying benefits in neurodegenerative diseases. These investigations have used both genetic and pharmacological approaches to manipulating this network. In prior studies of SOD1 aggregation, using cultured cell models, we had observed that the over-expression of the small heat shock chaperone αB-crys was sufficient to slow mutant SOD1 aggregation (Karch and Borchelt 2010). Additionally, we had observed that eliminating αB-crys expression in mutant SOD1 mice by targeted-gene-deletion produced a small, but statistically significant, acceleration in the age to paralysis (Karch and Borchelt 2010). Thus, we had anticipated that raising the levels of αB-crys in motor neurons could provide substantial benefit. Here, we used transgenic approaches to elevate the levels of αB-crys in the spinal neuroaxis of mice by 6 fold, with clear evidence of increased expression in motor neurons. Our analysis of motor neuron numbers in spinal cords of mice expressing αB-crys suggests that this small chaperone may be a survival factor that diminishes motor neuron loss that occurs during development, since these mice were found to have about 20% more motor neurons per section than littermate controls. This finding provides an indication that we managed to express this chaperone at levels that impacted neuronal survival. However, augmenting proteostatic function by elevating this specific chaperone was not sufficient to significantly delay the age at which mutant SOD1 mice become paralyzed or reduce the accumulation of misfolded SOD1 aggregates. Of these two findings, the latter is the most disappointing because our prior studies in cell culture had indicated that αB-crys could inhibit mutant SOD1 aggregation. However, there are clear differences between the two model systems in that in the cell model both mutant SOD1 and αB-crys are vastly over-expressed whereas in the mouse models the level of over-expression is high, but not to the extent that occurs in transiently-transfected cell models. Thus, although the cell data predict that αB-crys may have the potential to modulate mutant SOD1 aggregation, the mouse findings indicate little or no efficacy *in vivo*. Whether expression of a much higher level of αB-crys in spinal cord would attenuate mutant SOD1 aggregation is uncertain. We note that the steady-state levels of mutant SOD1 protein in the G93A and L126Z mice differ by at

least 1 order of magnitude. The lack of an effect in the G93A mice may be forgiven due to insufficient expression of αB-Crys, but the lack of an effect in the L126Z mice suggests that the level of expression required to achieve therapeutic benefit is potentially extraordinarily high. It is also possible that the cell model of aggregation, which involves processes occurring over 24- or 48- hour periods, simply does not predict processes *in vivo*, where events play out over weeks or months in very specialized cells. Overall, our data indicate that raising the levels of αB-crys in motor neurons, *in vivo*, by a substantial level is insufficient to slow the development of motor neuron disease or diminish the aggregation of mutant SOD1.

The predominant immunostaining for αB-crys in spinal cords of non-transgenic mice is in cells that morphologically classify as oligodendrocytes (Wang *et al.* 2005a) and the induced immunoreactivity in spinal cords of mutant SOD1 mice is in cells that morphologically resemble astrocytes (Karch and Borchelt 2010; Wang *et al.* 2005a). This distribution of immunoreactivity is consistent with *in situ* hybridization studies of αB-crys expression in brain. Strong *in situ* hybridization signals for this gene, provided on the Allen Brain Atlas, is in white matter tracts of the cortex and cerebellum {www.mouse.brain-map.org}, with a homogenous distribution of signal throughout the mid and hind brain (Figs. S6 & S7). Thus, normally, αB-crys is not highly expressed in neurons. In our PrP.αB-crys transgenic mice, we observe a strong immunoreactivity to αB-crys antibodies in large spinal motor neurons. Correlatively, we observe that mice expressing αB-crys have more ChAT positive motor neurons per section than nontransgenic littermates. Thus, we confirm that we have successfully raised the levels of this small chaperone in motor neurons by a substantial degree. On face value, our data indicate that augmenting proteostatic function by chronically increasing the level of αB-crys by ~6-fold in spinal cord is insufficient to attenuate the misfolding and aggregation of mutant SOD1 or delay the onset of paralysis. It is possible that raising the levels by a greater degree would ultimately reproduce the effects on mutant SOD1 aggregation seen in cell culture models, but it is also possible that the cell culture data simply do not accurately predict *in vivo* outcomes where the time scales of protein aggregation are much longer.

Supplementary Material

Refer to Web version on PubMed Central for supplementary material.

Acknowledgements

We thank Drs. J.P. Whitelegge, David Eisenberg, and Joan Valentine for helpful discussions through the course of these experiments. We thank Matthew S Collins for his assistance in tissue sectioning. This work was supported by a grant from the National Institutes of Neurological Disease and Stroke (P01 NS049134 – Program Project). All experiments were conducted in compliance with the ARRIVE guidelines.

Abbreviations

αB-crys	αB-crystallin
ALS	amyotrophic lateral sclerosis

BNGE	Blue Native Gel Electrophoresis
ChAT	choline acetyl transferase
DTg	bigenic mice co-expressing αB-crys and mutant SOD1
HSPs	Heat shock proteins
Human SOD1	hSOD1
Line 45	mice that express the L126Z mutant from a specific line designated Line 45
NTg	non-transgenic
P2	centrifugation pellet fraction #2
PBS	phosphate buffered saline
PBS-T	PBS with 0.1% Tween 20
PrP	prion protein
S1	supernatant fraction #1
S2	supernatant fraction #2
SDS-PAGE	sodium dodecyl sulfate polyacrylamide gel electrophoresis
SOD1	superoxide dismutase 1
Z104	mice that express the αB-crys protein from a specific line designated Z104

References

Akerfelt M, Morimoto RI, Sistonen L. Heat shock factors: integrators of cell stress, development and lifespan. Nat. Rev. Mol. Cell Biol. 2010; 11:545–555. [PubMed: 20628411]

Balch WE, Morimoto RI, Dillin A, Kelly JW. Adapting proteostasis for disease intervention. Science. 2008; 319:916–919. [PubMed: 18276881]

Batulan Z, Shinder GA, Minotti S, He BP, Doroudchi MM, Nalbantoglu J, Strong MJ, Durham HD. High threshold for induction of the stress response in motor neurons is associated with failure to activate HSF1. J. Neurosci. 2003; 23:5789–5798. [PubMed: 12843283]

Borchelt DR, Davis J, Fischer M, Lee MK, Slunt HH, Ratovitsky T, Regard J, Copeland NG, Jenkins NA, Sisodia SS, Price DL. A vector for expressing foreign genes in the brains and hearts of transgenic mice. Genet. Anal. 1996; 13:159–163. [PubMed: 9117892]

Bosco DA, Morfini G, Karabacak NM, Song Y, Gros-Louis F, Pasinelli P, Goolsby H, Fontaine BA, Lemay N, McKenna-Yasek D, Frosch MP, Agar JN, Julien JP, Brady ST, Brown RH Jr. Wild-type and mutant SOD1 share an aberrant conformation and a common pathogenic pathway in ALS. Nat. Neurosci. 2010; 13:1396–1403. [PubMed: 20953194]

Brown HH, Borchelt DR. Analysis of Mutant SOD1 Electrophoretic Mobility by Blue Native Gel Electrophoresis; Evidence for Soluble Multimeric Assemblies. PLoS One. 2014; 9:e104583. [PubMed: 25121776]

Bruijn LI, Becher MW, Lee MK, Anderson KL, Jenkins NA, Copeland NG, Sisodia SS, Rothstein JD, Borchelt DR, Price DL, Cleveland DW. ALS-linked SOD1 mutant G85R mediates damage to astrocytes and promotes rapidly progressive disease with SOD1-containing inclusions. Neuron. 1997; 18:327–338. [PubMed: 9052802]

Deng HX, Chen W, Hong ST, Boycott KM, gorrie GH, Siddique N, Yang Y, Fecto F, Shi Y, Zhai H, Jiang H, Hirano M, Rampersaud E, Jansen GH, Donkervoort S, Bigio EH, Brooks BR, Ajroud K, Sufit RL, Haines JL, Mugnaini E, Pericak-Vance MA, Siddique T. Mutations in UBQLN2 cause dominant X-linked juvenile and adult-onset ALS and ALS/dementia. Nature. 2011; 477:211–215. [PubMed: 21857683]

Deng HX, Zhai H, Bigio EH, Yan J, Fecto F, Ajroud K, Mishra M, Ajroud-Driss S, Heller S, Sufit R, Siddique N, Mugnaini E, Siddique T. FUS-immunoreactive inclusions are a common feature in sporadic and non-SOD1 familial amyotrophic lateral sclerosis. Ann. Neurol. 2010; 67:739–748. [PubMed: 20517935]

Fecto F, Siddique T. Making connections: pathology and genetics link amyotrophic lateral sclerosis with frontotemporal lobe dementia. J. Mol. Neurosci. 2011; 45:663–675. [PubMed: 21901496]

Forsberg K, Jonsson PA, Andersen PM, Bergemalm D, Graffmo KS, Hultdin M, Jacobsson J, Rosquist R, Marklund SL, Brannstrom T. Novel antibodies reveal inclusions containing non-native SOD1 in sporadic ALS patients. PLoS. ONE. 2010; 5:e11552. [PubMed: 20644736]

Frydman J. Folding of newly translated proteins in vivo: the role of molecular chaperones. Annu. Rev. Biochem. 2001; 70:603–647. [PubMed: 11395418]

Gould TW, Buss RR, Vinsant S, Prevette D, Sun W, Knudson CM, Milligan CE, Oppenheim RW. Complete dissociation of motor neuron death from motor dysfunction by Bax deletion in a mouse model of ALS. J. Neurosci. 2006; 26:8774–8786. [PubMed: 16928866]

Grad LI, Yerbury JJ, Turner BJ, Guest WC, Pokrishevsky E, O'Neill MA, Yanai A, Silverman JM, Zeineddine R, Corcoran L, Kumita JR, Luheshi LM, Yousefi M, Coleman BM, Hill AF, Plotkin SS, Mackenzie IR, Cashman NR. Intercellular propagated misfolding of wild-type Cu/Zn superoxide dismutase occurs via exosome-dependent and -independent mechanisms. Proc. Natl. Acad. Sci. U. S. A. 2014; 111:3620–3625. [PubMed: 24550511]

Gurney ME, Pu H, Chiu AY, Dal Canto MC, Polchow CY, Alexander DD, Caliendo J, Hentati A, Kwon YW, Deng HX. Motor neuron degeneration in mice that express a human Cu, Zn superoxide dismutase mutation. Science. 1994; 264:1772–1775. [PubMed: 8209258]

Han S, Choi JR, Soon SK, Kang SJ. Resveratrol upregulated heat shock proteins and extended the survival of G93A-SOD1 mice. Brain Res. 2012; 1483:112–117. [PubMed: 23000195]

Johnston JA, Dalton MJ, Gurney ME, Kopito RR. Formation of high molecular weight complexes of mutant Cu, Zn-superoxide dismutase in a mouse model for familial amyotrophic lateral sclerosis. Proc. Natl. Acad. Sci. U. S. A. 2000; 97:12571–12576. [PubMed: 11050163]

Jonsson PA, Ernhill K, Andersen PM, Bergemalm D, Brannstrom T, Gredal O, Nilsson P, Marklund SL. Minute quantities of misfolded mutant superoxide dismutase-1 cause amyotrophic lateral sclerosis. Brain. 2004; 127:73–88. [PubMed: 14534160]

Kaarniranta K, Oksala N, Karjalainen HM, Suuronen T, Sistonen L, Helminen HJ, Salminen A, Lammi MJ. Neuronal cells show regulatory differences in the hsp70 gene response. Brain Res. Mol. Brain Res. 2002; 101:136–140. [PubMed: 12007842]

Kalmar B, Novoselov S, Gray A, Cheetham ME, Margulis B, Greensmith L. Late stage treatment with arimoclomol delays disease progression and prevents protein aggregation in the SOD1 mouse model of ALS. J. Neurochem. 2008; 107:339–350. [PubMed: 18673445]

Karch CM, Borchelt DR. An examination of alpha B-crystallin as a modifier of SOD1 aggregate pathology and toxicity in models of familial amyotrophic lateral sclerosis. J. Neurochem. 2010; 113:1092–1100. [PubMed: 20067574]

Karch CM, Prudencio M, Winkler DD, Hart PJ, Borchelt DR. Role of mutant SOD1 disulfide oxidation and aggregation in the pathogenesis of familial ALS. Proc. Natl. Acad. Sci. U. S. A. 2009; 106:7774–7779. [PubMed: 19416874]

Kieran D, Kalmar B, Dick JR, Riddoch-Contreras J, Burnstock G, Greensmith L. Treatment with arimoclomol, a coinducer of heat shock proteins, delays disease progression in ALS mice. Nat. Med. 2004; 10:402–405. [PubMed: 15034571]

Kozak M. At least six nucleotides preceding the AUG initiator codon enhance translation in mammalian cells. J. Mol. Biol. 1987; 196:947–950. [PubMed: 3681984]

Kumar LV, Rao CM. Domain swapping in human alpha A and alpha B crystallins affects oligomerization and enhances chaperone-like activity. J. Biol. Chem. 2000; 275:22009–22013. [PubMed: 10896951]

Lin PY, Simon SM, Koh WK, Folorunso O, Umbaugh CS, Pierce A. Heat shock factor 1 over-expression protects against exposure of hydrophobic residues on mutant SOD1 and early mortality in a mouse model of amyotrophic lateral sclerosis. Mol. Neurodegener. 2013; 8 43-1326-8-43.

Liu J, Shinobu LA, Ward CM, Young D, Cleveland DW. Elevation of the Hsp70 chaperone does not effect toxicity in mouse models of familial amyotrophic lateral sclerosis. J. Neurochem. 2005; 93:875–882. [PubMed: 15857390]

Lowe J, Mayer RJ, Landon M. Ubiquitin in neurodegenerative diseases. Brain Pathol. 1993; 3:55–65. [PubMed: 8269084]

Marber MS, Mestril R, Chi SH, Sayen MR, Yellon DM, Dillmann WH. Overexpression of the rat inducible 70-kD heat stress protein in a transgenic mouse increases the resistance of the heart to ischemic injury. J. Clin. Invest. 1995; 95:1446–1456. [PubMed: 7706448]

Morimoto RI. Proteotoxic stress and inducible chaperone networks in neurodegenerative disease and aging. Genes Dev. 2008; 22:1427–1438. [PubMed: 18519635]

Mulligan VK, Chakrabartty A. Protein misfolding in the late-onset neurodegenerative diseases: common themes and the unique case of amyotrophic lateral sclerosis. Proteins. 2013; 81:1285–1303. [PubMed: 23508986]

Oza J, Yang J, Chen KY, Liu AY. Changes in the regulation of heat shock gene expression in neuronal cell differentiation. Cell Stress Chaperones. 2008; 13:73–84. [PubMed: 18347944]

Pavlik A, Aneja IS. Cerebral neurons and glial cell types inducing heat shock protein Hsp70 following heat stress in the rat. Prog. Brain Res. 2007; 162:417–431. [PubMed: 17645930]

Pavlik A, Aneja IS, Lexa J, Al-Zoabi BA. Identification of cerebral neurons and glial cell types inducing heat shock protein Hsp70 following heat stress in the rat. Brain Res. 2003; 973:179–189. [PubMed: 12738061]

Prudencio M, Borchelt DR. Superoxide dismutase 1 encoding mutations linked to ALS adopts a spectrum of misfolded states. Mol. Neurodegener. 2011; 6:77. [PubMed: 22094223]

Prudencio M, Hart PJ, Borchelt DR, Andersen PM. Variation in aggregation propensities among ALS-associated variants of SOD1: correlation to human disease. Hum. Mol. Genet. 2009; 18:3217–3226. [PubMed: 19483195]

Rangaraju S, Madorsky I, Pileggi JG, Kamal A, Notterpek L. Pharmacological induction of the heat shock response improves myelination in a neuropathic model. Neurobiol. Dis. 2008; 32:105–115. [PubMed: 18655835]

Ratovitski T, Corson LB, Strain J, Wong P, Cleveland DW, Culotta VC, Borchelt DR. Variation in the biochemical/biophysical properties of mutant superoxide dismutase 1 enzymes and the rate of disease progression in familial amyotrophic lateral sclerosis kindreds. Hum. Mol. Genet. 1999; 8:1451–1460. [PubMed: 10400992]

Schagger H, von Jagow G. Blue native electrophoresis for isolation of membrane protein complexes in enzymatically active form. Anal. Biochem. 1991; 199:223–231. [PubMed: 1812789]

Sherman MY, Goldberg AL. Cellular defenses against unfolded proteins: a cell biologist thinks about neurodegenerative diseases. Neuron. 2001; 29:15–32. [PubMed: 11182078]

Vogel P, Dux E, Wiessner C. Effect of heat shock on neuronal cultures: importance of protein synthesis and HSP72 induction for induced tolerance and survival. Metab. Brain Dis. 1997; 12:203–217. [PubMed: 9346469]

Wang J, Slunt H, Gonzales V, Fromholt D, Coonfield M, Copeland NG, Jenkins NA, Borchelt DR. Copper-binding-site-null SOD1 causes ALS in transgenic mice: aggregates of non-native SOD1 delineate a common feature. Hum. Mol. Genet. 2003; 12:2753–2764. [PubMed: 12966034]

Wang J, Xu G, Borchelt DR. High molecular weight complexes of mutant superoxide dismutase 1: age- dependent and tissue-specific accumulation. Neurobiol. Dis. 2002a; 9:139–148. [PubMed: 11895367]

Wang J, Xu G, Gonzales V, Coonfield M, Fromholt D, Copeland NG, Jenkins NA, Borchelt DR. Fibrillar inclusions and motor neuron degeneration in transgenic mice expressing superoxide

dismutase 1 with a disrupted copper-binding site. Neurobiol. Dis. 2002b; 10:128–138. [PubMed: 12127151]

Wang J, Xu G, Li H, Gonzales V, Fromholt D, Karch C, Copeland NG, Jenkins NA, Borchelt DR. Somatodendritic accumulation of misfolded SOD1-L126Z in motor neurons mediates degeneration: {alpha}B-crystallin modulates aggregation. Hum. Mol. Genet. 2005a; 14:2335–2347. [PubMed: 16000321]

Wang J, Xu G, Slunt HH, Gonzales V, Coonfield M, Fromholt D, Copeland NG, Jenkins NA, Borchelt DR. Coincident thresholds of mutant protein for paralytic disease and protein aggregation caused by restrictively expressed superoxide dismutase cDNA. Neurobiol. Dis. 2005b; 20:943–952. [PubMed: 16046140]

Watanabe M, Dykes-Hoberg M, Culotta VC, Price DL, Wong PC, Rothstein JD. Histological Evidence of Protein Aggregation in Mutant SOD1 Transgenic Mice and in Amyotrophic Lateral Sclerosis Neural Tissues. Neurobiol. Dis. 2001; 8:933–941. [PubMed: 11741389]

Xu G, Ayers JI, Roberts BL, Brown H, Fromholt S, Green C, Borchelt DR. Direct and indirect mechanisms for wild-type SOD1 to enhance the toxicity of mutant SOD1 in bigenic transgenic mice. Hum. Mol. Genet. 2014

Yang J, Oza J, Bridges K, Chen KY, Liu AY. Neural differentiation and the attenuated heat shock response. Brain Res. 2008; 1203:39–50. [PubMed: 18316066]

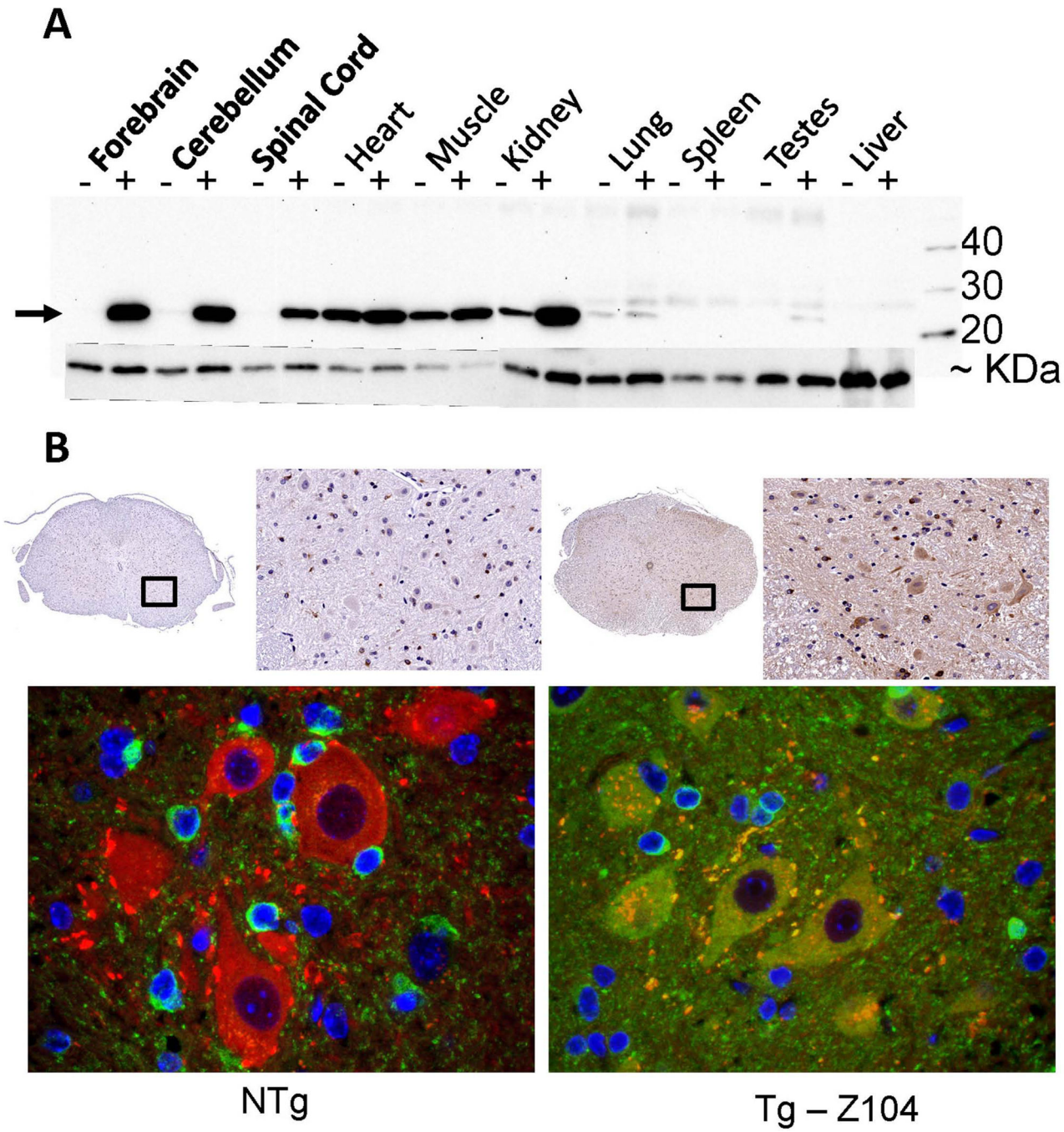

Fig. 1.

Expression of αB-crys in transgenic mice. A) Immunoblot showing that αB-crys is normally expressed at low levels in the central nervous system and that the levels are substantially raised in transgenic mice from line Z104 that express human αB-crys (see Fig. S2). The amount of αB-crys was also clearly increased in kidney, but expression of the transgene in muscle or heart, which is known to occur (Borchelt *et al.* 1996), did not obviously increase the levels of this chaperone. An arrow marks the position of αB-crys, whereas the lower band is mouse endogenous SOD1 that was used as a loading control. B)

Immunohistochemistry was used to detect αB-crys (green) and choline acetyl transferase (ChAT)(red) expression in spinal cord. In the Z104 transgenic animals, more intense αB-crys immunoreactivity was detected throughout the spinal cord with obvious staining of large neuronal cells in the ventral horn. The images shown are representative of data from at least 3 animals per genotype with at least 9 tissue sections, from different spinal cord levels, per animal. All motor neurons in the ventral horn appear to express αB-crys in the Z104 mice.

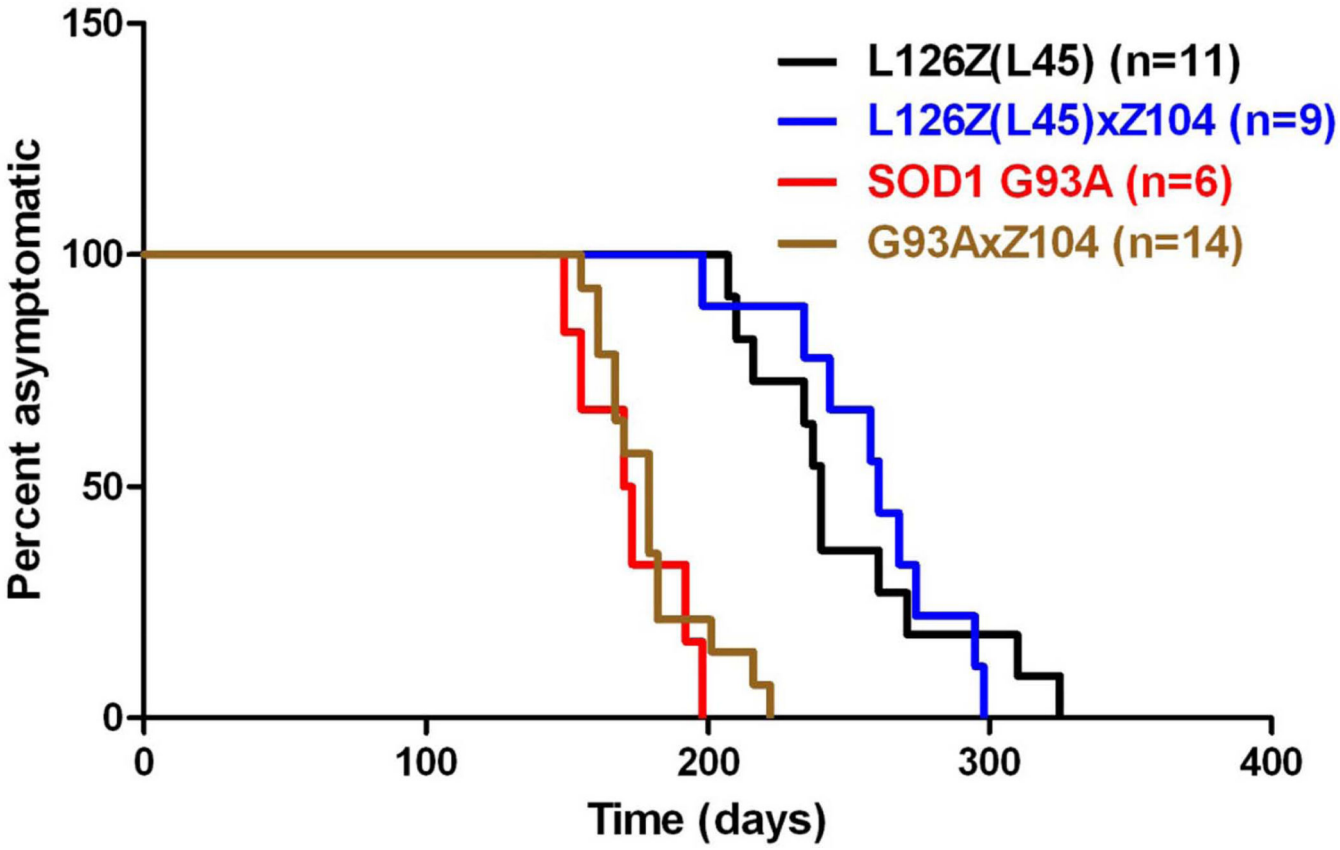

Fig. 2.

Co-expression of αB-crys does not markedly delay the age to paralysis in transgenic mice expressing the G93A or L126Z variants of mutant SOD1. Software that is used in plotting survival was used to illustrate the ages at which mice expressing G93A SOD1 alone (G93A), L126Z SOD1 alone (Line 45 – abbrev L45), bigenic G93A/αB-crys, and bigenic L45/αB-crys reach a humane endpoint of hindlimb paralysis. There were no significant differences between mice expressing mutant SOD1 alone, and bigenic mice co-expressing αB-crys.

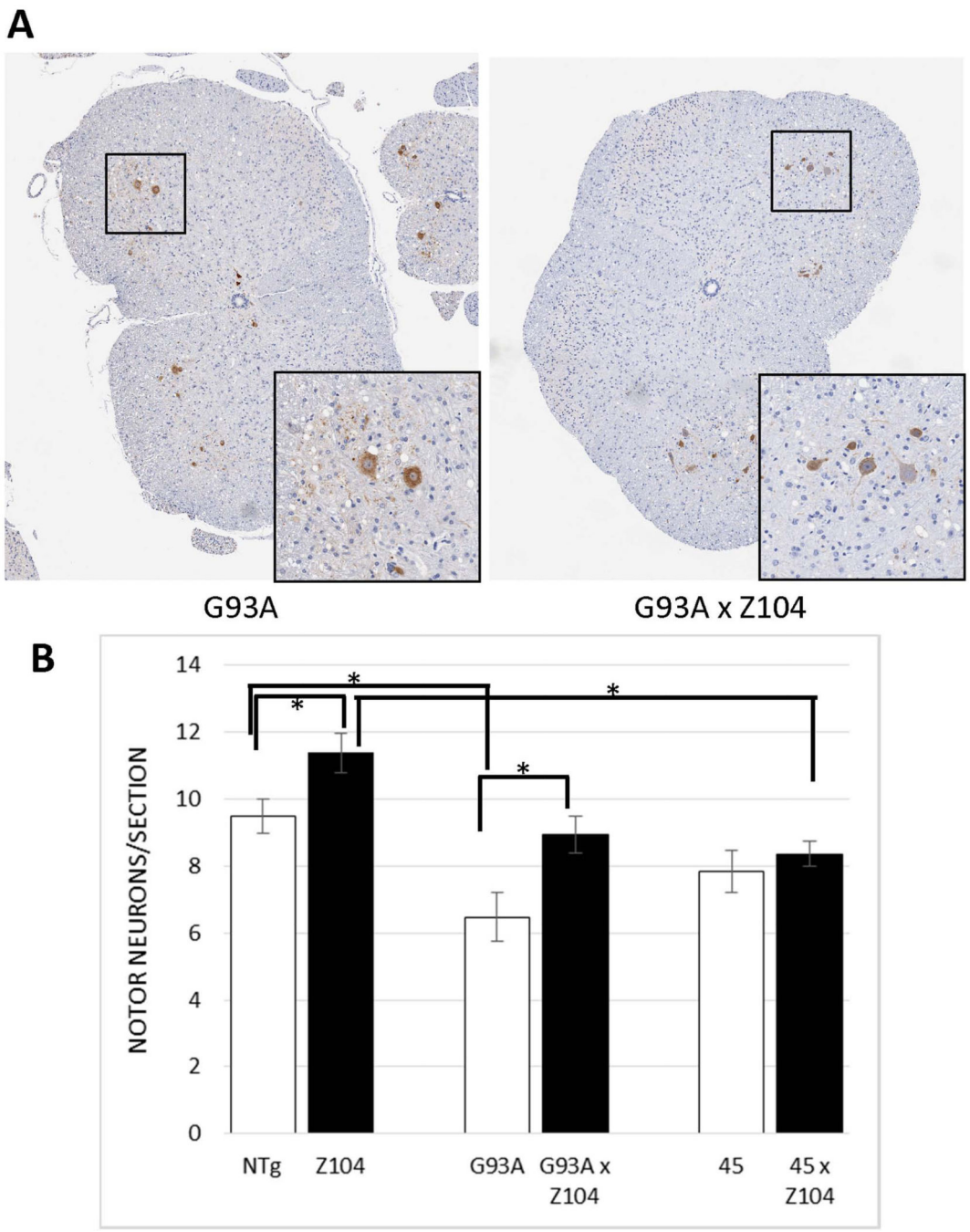

Fig. 3.

Estimations of ChAT positive motor neurons in the spinal cords of monogenic and bigenic transgenic mice. Randomly selected spinal cord tissue sections from different levels of the cord were stained with ChAT antibody to identify motor neurons of the ventral horn. The number of ChAT immunoreactive motor neurons in spinal sections from at least 2–3 slides per animal, with each slide containing 2–4 spinal cord coronal sections, were counted by two people independently that were blind to genotypes. Data were statistically analyzed as described in Materials and Methods (see Results for p values). The brackets identify data

sets that were determined to be statistically different (marked by *). The numbers of mice analyzed for each genotype were as follows: NTg (n=8), Z104 (n=15), hSOD1-L126Z (Line45) (n=9), bigenic L45/αB-crys (n=9), hSOD1-G93A (n=5), bigenic G93A/αB-crys (n=10). The error bar notes the standard error of the mean (SEM).

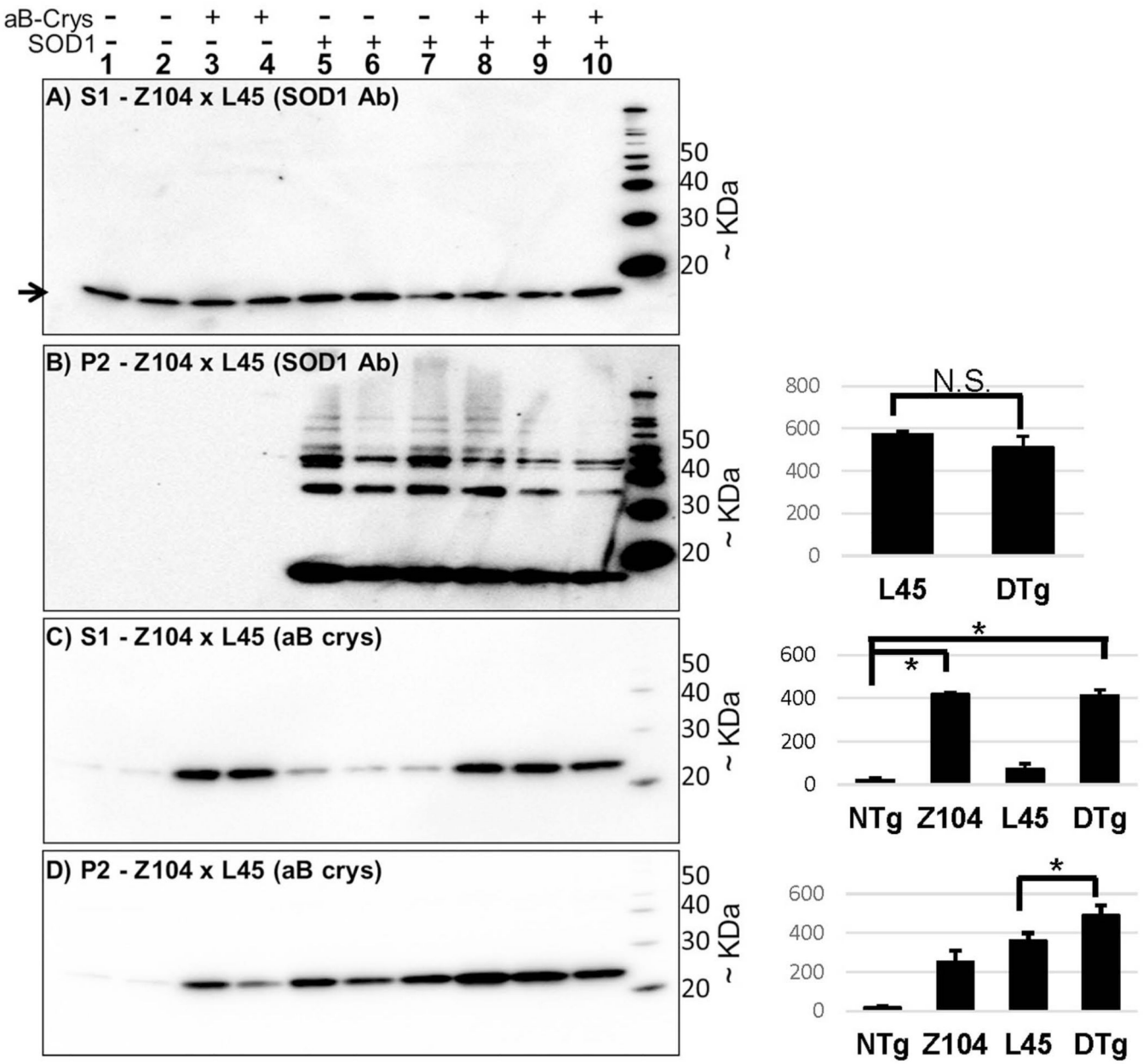

Fig. 4.

Analysis of detergent soluble and insoluble forms of SOD1 and αB-crys in L126Z (Line 45) × αB-crys (Z104) transgenic mice. A and B) Immunoblots of NP40 soluble (S1) and insoluble (P2) fractions, respectively, with an antibody raised against the purified SOD1 protein (Ratovitski *et al.* 1999). The major immunoreactive protein seen in panel A is endogenous mouse SOD1. The higher molecular weight bands seen in lanes 6–10 of panel B are a combination of ubiquitinated L126Z protein and SDS-resistant dimers and multimers (Wang *et al.* 2005a). C and D) Immunoblot of NP40 soluble (S1) and insoluble (P2) fractions, respectively, with an antibody to αB-crys. The bar graphs to the right of each panel document quantification of the relevant bands in each blot. The bar graph to the right of panel (B) shows quantification of the major SOD1 reactive band in the blot which

migrates at the expected size for L126Z hSOD1 (~15 kDa). DTg = bigenic Z104/L45 mice. The error bar notes the standard deviation (SD) (n=3 for each genotype). Statistical comparisons of the data marked by brackets used the student's t-test (2-tailed, unpaired). Data that were statistically different are marked by (*), see Results for p values.

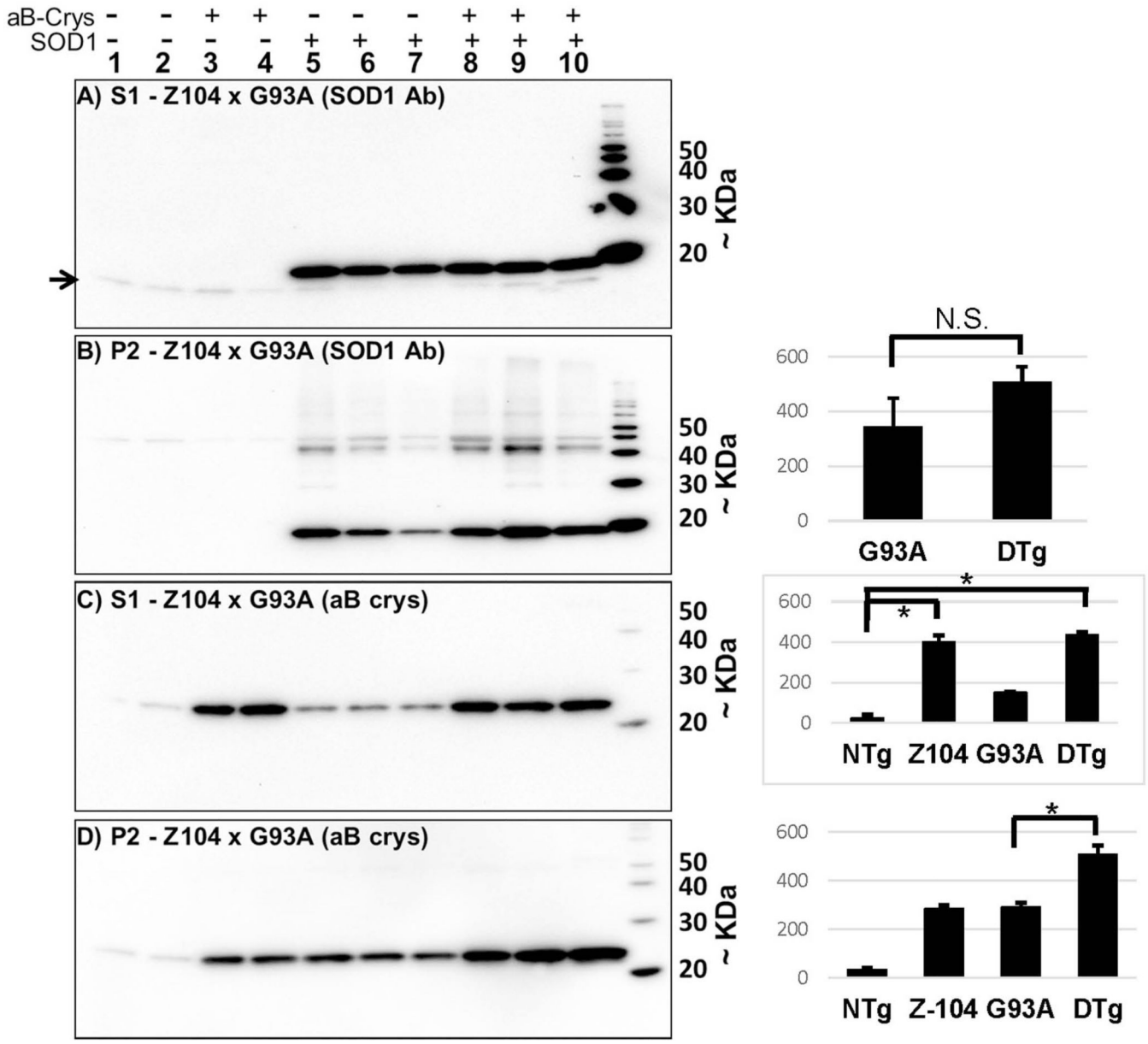

Fig. 5.

Analysis of detergent soluble and insoluble forms of SOD1 and αB-crys in G93A × αB-crys (Z104) transgenic mice. A and B) Immunoblots of NP40 soluble (S1) and insoluble (P2) fractions, respectively, with the SOD1 antibody. The low level of endogenous mouse SOD1, compared to the expressed G93A protein is evident in all lanes, position of mouse SOD1 marked by arrow. The higher molecular weight bands seen in lanes 6–10 of panel B are a combination of ubiquitinated G93A protein and SDS-resistant dimers (Wang *et al.* 2003). C and D) Immunoblot of NP40 soluble (S1) and insoluble (P2) fractions, respectively, with an antibody to αB-crys. The bar graph to the right of panel (B) shows quantification of the major SOD1 reactive band in the blot which migrates at the expected size for G93A hSOD1 (~20 kDa). DTg = bigenic Z104/G93A mice. The error bar notes the standard deviation (SD) (n=3 for each genotype). Statistical comparisons of the data marked by brackets used the

student’s t-test (2-tailed, unpaired). Data that were statistically different are marked by (*), see Results for p values.

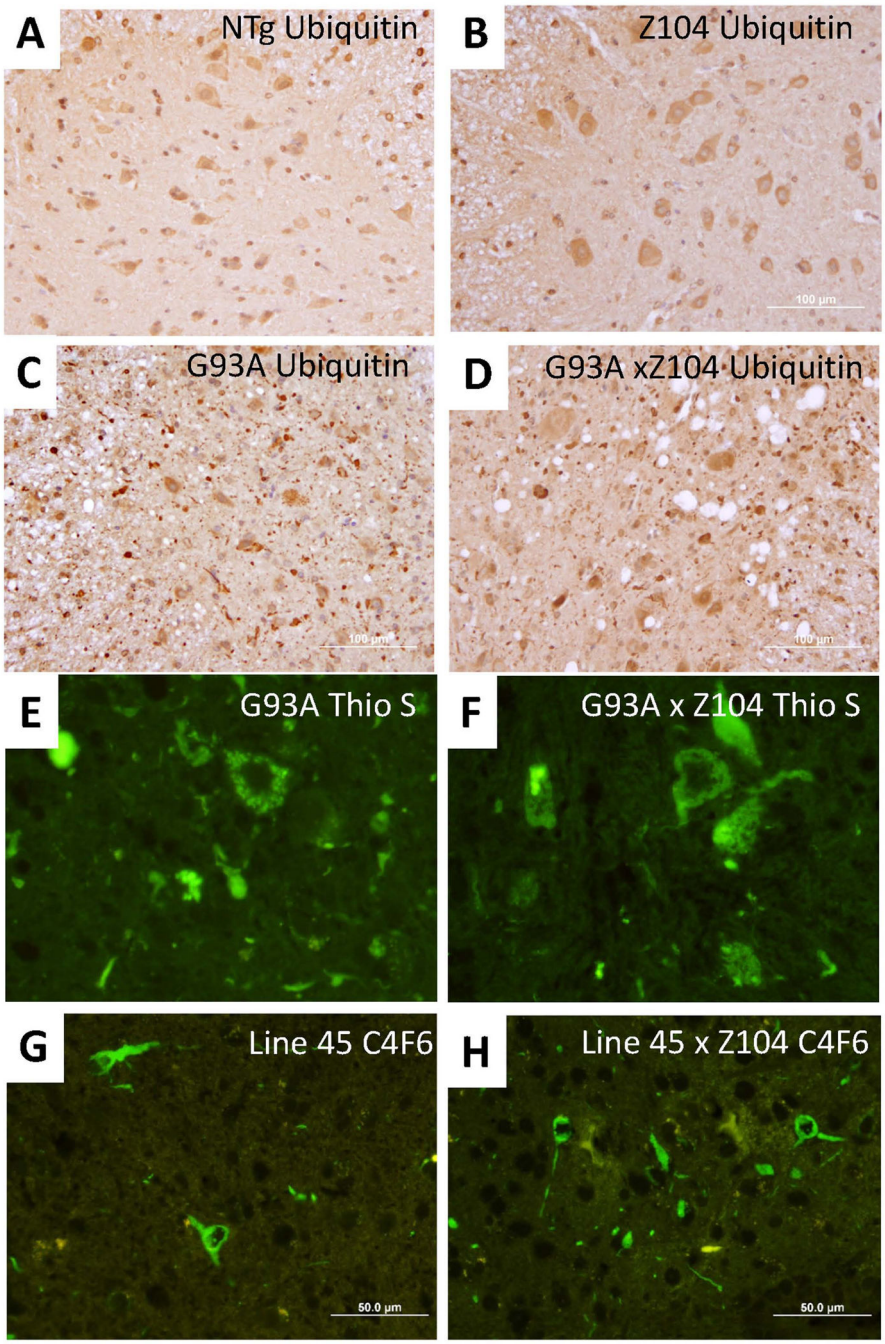

Fig. 6.

Comparison of pathology in G93A × αB-crys (Z104) transgenic mice. A–D) Representative examples of immunostains with ubiquitin antibody in non-transgenic mice (NTg), αB-crys (Z104) transgenic mice, G93A alone mice, and bigenic G93A/αB-crys mice, respectively. Note the prominent vacuolar pathology in the paralyzed mice expressing G93A SOD1 and the small punctate neuropil structures. These structures are as abundant, if not more so, in the paralyzed bigenic mice. E and F) Representative examples of thioflavin-S positive inclusions in G93A and G93A/αB-crys bigenic mice. There was no obvious decrease in the

frequency of thioflavin positive structures in the bigenic mice. G and H) Representative examples of C4F6 positive inclusions in L126Z (Line 45) and bigenic L126Z/αB-crys bigenic mice. There was no obvious decrease in the frequency of C4F6 immunoreactive positive structures in the bigenic mice. The images were captured by epifluorsecence microscope at 40×. The images shown are representative of data from at least 3 animals per genotype with at least 9 spinal cord sections per animal, from different spinal cord levels.

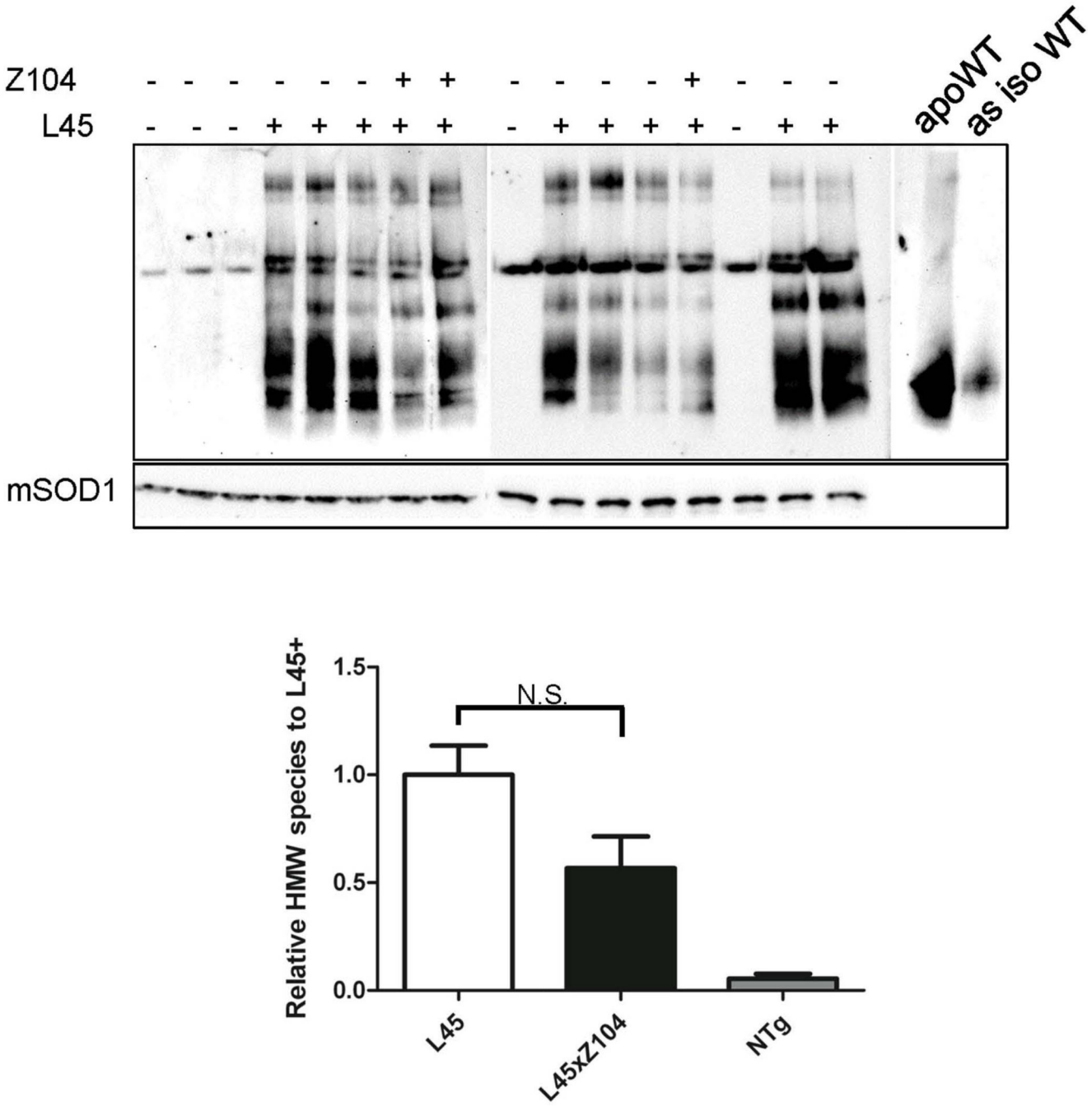

Fig. 7.

Co-expression of αB-crys with mutant SOD1 does not specifically diminish the amount of slowly migrating SOD1 immunoreactivity in BN-gels. HEK 293FT cells were transiently transfected with WT or mutant SOD1 alone or in co-transfection with vectors to express αB-crys. Immunoblots of BN-gels of cell lysates were probed with the hSOD1 antibody. Portions of the same lysates were analyzed by SDS-PAGE and immunoblotting with the hSOD1 antibody. Co-expression of αB-crys appeared to reduce the intensity of SOD1 reactivity on BN-gels (A and B), but did not collapse the oligomeric immunoreactive species

into a species migrating as the expected size for monomeric L126Z-hSOD1, and the difference in total mutant SOD1 immunoreactivity between Line 45 and Lin 45 × Z104 mice was not statistically significant (Students' s t-Test). The error bar notes the standard deviation (SD).